Cardiovascular Toxicology (2019) 19:306–320
https://doi.org/10.1007/s12012-019-09512-1

Acute and Subacute Effects of Low Versus High Doses of Standardized *Panax ginseng* Extract on the Heart: An Experimental Study

Hakan Parlakpinar[1] · Onural Ozhan[1] · Necip Ermis[2] · Nigar Vardi[3] · Yilmaz Cigremis[4] · Lokman H. Tanriverdi[1] · Cemil Colak[5] · Ahmet Acet[1]

Published online: 21 March 2019

Abstract

Panax ginseng is commonly used in Chinese medicine and Western herbal preparations. However, it has also been recently noted to be associated with some cardiac pathologies-including cardiogenic shock due to acute anterior myocardial infarction, trans-ischemic attack, and stent thrombosis. This study was aimed to elucidate acute and subacute effects of the low and high doses of standardized *Panax ginseng* extract (sPGe) on cardiac functions. Rats were randomly assigned to control group, acute low-dose group (ALD), subacute low-dose group (SALD), acute high-dose group (AHD), and subacute high-dose group (SAHD). The cardiac effects of sPGe were evaluated using hemodynamic, biochemical, echocardiographic, genetic, and immunohistopathologic parameters. Mean blood pressures were significantly lower in all sPGe-treated groups compared with the control group. Troponin I and myoglobin levels were increased in the SALD, AHD, and SAHD groups. Mitral E-wave velocity was reduced after sPGe administration in all the groups. Acidophilic cytoplasm and pyknotic nucleus in myocardial fibers were observed in AHD and SAHD groups. Cu/Zn-SOD1 gene expressions were significantly higher in the sPGe-treated groups whereas caveolin 1 and VEGF-A gene expressions were not changed. According to our results, sPGe may have a potential effect to cause cardiac damage including diastolic dysfunction, heart failure with preserved ejection fraction, and reduction of blood pressure depending on the dose and duration of usage. Healthcare professionals must be aware of adverse reactions stemming from the supplementation use, particularly with cardiac symptoms.

Keywords *Panax ginseng* · Cardiotoxicity · Standardized extract · Heart · Rats · Heart failure with preserved ejection fraction

Abbreviations

sPGe	Standardized *Panax ginseng* extract
ALD	Acute low dose
SALD	Subacute low dose
AHD	Acute high dose
SAHD	Subacute high dose
AV	Atrioventricular
AA	Diameter of ascending aorta
LA	Diameter of left atrium
IVSt	Interventricular septal thickness in diastole
LVED	Left ventricular end-diastolic diameter
LVES	Left ventricular end-systolic diameter
EF	Ejection fraction
FS	Fractional shortening
E/A	Peak velocity of E-wave/peak velocity of A-wave

This study was presented at the 24th National Pharmacology Congress at Trabzon, Turkey, Nov, 2017.

Handling Editor: Lorraine Chalifour.

Electronic supplementary material The online version of this article (https://doi.org/10.1007/s12012-019-09512-1) contains supplementary material, which is available to authorized users.

✉ Hakan Parlakpinar
hakan.parlakpinar@inonu.edu.tr

[1] Department of Medical Pharmacology, Faculty of Medicine, Inonu University, Malatya, Turkey

[2] Department of Cardiology, Faculty of Medicine, Inonu University, Malatya, Turkey

[3] Department of Histology and Embryology, Faculty of Medicine, Inonu University, Malatya, Turkey

[4] Department of Medical Biology and Genetics, Faculty of Medicine, Inonu University, Malatya, Turkey

[5] Department of Biostatistics and Medical Informatics, Faculty of Medicine, Inonu University, Malatya, Turkey

EDT E-wave deceleration time
CAV1 Caveolin 1

Introduction

Before the advent of Western medicine and its pharmacopeia of synthetic drugs, there were medicinal plants. Plants that had been used for various purposes for thousands of years were seen in Evers papyrus in 1550 BC in Egypt, and their use had been also mentioned in Hippocratic Greek Corpus [1]. Later, during the 1800s and early 1900s, the knowledge of herbal medicine was passed down from one generation to the next. Despite the development of medicine and medical pharmacology in the modern-era, usage of many plants and herbs has been increasing day by day by people all over the world [2].

Ginseng belongs to the *Araliaceae* family and has several different species, namely *Panax ginseng, Panax japonicus*, and *Panax quinquefolius*, among others, which differ in both physical appearance and chemical constitutions [3]. Two major species of ginseng that have been well documented in history and used as therapeutic agents are *Panax ginseng C.A. Meyer* (named after the Russian botanist C.A. Meyer, who identified and isolated the different ginseng species in 1842) in China and Korea. Karmazyn et al. have recently reported that "The popularity of ginseng as a medicinal drug, not to mention a high trade commodity item, after its introduction into New France in North America in the early 1700s, however, was quite remarkable. By late 1700, there were several accounts as well as refuted claims of the therapeutic effects of ginseng, although these were generally based on individual cases or the effects experienced by the researcher or physician themselves." [4].

Recently, there are many clinical and experimental publications in the literature about cardiotoxic effects taking place due to the use of *Panax ginseng* and its compounds [5–8]. Vuksan et al. showed that low doses of Korean red ginseng have an antihypertensive effect compared to its high doses in a randomized controlled clinical trial study [9]. In addition, the blood pressure lowering activity of *Panax ginseng* is due to the promotion of vascular endothelial cell-derived nitric oxide (NO) secretion [10, 11]. *Panax ginseng* has been used for the treatment of heart failure and to protect tissues from damage when an organism is under stress [12]. These attributes show the pure benefit of *Panax ginseng* on the cardiovascular system. Unfortunately, there are many cases in the literature that show the cardiotoxic effects of *Panax ginseng*. Some published *Panax ginseng*-related adverse cardiovascular events, and subjects presented with acute International Normalized Ratio (INR) elevation [13], QT prolongation [14], cardiogenic shock due to acute anterior myocardial infarction [15], stent thrombosis, trans-ischemic attack [16], and acute diffuse pulmonary embolism [17]. There are a few studies that evaluated the potential cardiovascular toxic effects of *Panax ginseng* over the last few years, but the related literature and the mechanism are inconclusive [18].

Currently, 60 ginsenosides approximately have been isolated and identified, and the various methods of separation and analysis were well reviewed, and each has a different pharmacologic effect(s) and mechanism(s) of action [19]. The most studied ginsenosides in the recent literature are Rb1, Rg1, Rg3, Re, and Rd components. Wu et al. [20] investigated the influence of Rb1 on myocardial ischemia and reperfusion injury in diabetic rats induced by streptozotocin. According to their results, Rb1 reduced infarct size, cardiomyocyte apoptosis, and caspase-3 activity compared to the untreated animals; effects of Rb1 were blocked by wortmannin, a specific PI3K inhibitor. Also, Jiang et al. [21] studied preventive and therapeutic effects of Rb1 on monocrotaline-induced right ventricular hypertrophy, and Rb1 significantly decreased hypertrophic reactions, expression of arterial natriuretic peptide mRNA, calcineurin, nuclear factor of activated T-lymphocyte-3, and GATA4, a transcription factor that is expressed in the myocardium and has been implicated in the differentiation of cardiac myocytes in both therapeutic groups. Deng et al. [22] investigated the influence of Rg1 on left ventricular hypertrophy induced by abdominal aorta coarctation and found that Rg1 significantly ameliorated left ventricular hypertrophy in a dose-dependent manner showing best results at 15 mg/kg/day; the expression of MAP kinase phosphatase 1 was increased by Rg1; mRNA expression of atrial natriuretic peptide was reduced significantly; and expressions of calcineurin and kinase 1 were decreased significantly. Re component significantly inhibited cardiomyocyte apoptosis and inhibited the expression of the pro-apoptotic Bax gene but did not influence the expression of Bcl/2, thus resulting in an increase of the ratio of Bcl-2/Bax on myocardial ischemia/reperfusion in rats [23]. In another study, apoE knockout mice were used for the investigation of the effect of Rd on atherosclerosis, and Rd (20 mg/kg/day i.p. preventive and therapeutic) reduced significantly the atherosclerotic plaque areas, oxidized LDL uptake and thapsigargin, and 1-oleoyl-2-acetyl-glycerol-induced Ca^{2+} influx in macrophages; increased levels of lipoproteins and blood lipids were not changed by Rd ginsenoside [24].

Based on those clinical and basic science reports, this article focuses on the acute and subacute cardiac effects of low and high doses of standardized *Panax ginseng* extract (sPGe) in an experimental study.

Methods

Study Design

In this study, we used standardized *Panax ginseng C.A. Meyer* dry extract herbal reference standards (HRS), which were already prepared according to the specifications described in the Panax ginseng monograph of the 7th edition European Pharmacopoeia. The extract had been produced from *Panax ginseng* that contains minimum 4% of the sum of ginsenosides Rb1, Rb2, Rc, Rd, Re, Rf, Rg1, and Rg2, expressed as ginsenoside Rb1 ($C_{54}H_{92}$, O_{23}; M_r1109) (dried extract). As mentioned, the herbal reference standard of the herbal product with Y0001029 code "Dry Ginseng Extract" is described in detail in the monograph. The extract is produced from the herbal drug by a suitable procedure using a hydroalcoholic solvent equivalent in strength to ethanol (35–90% V/V). The standardized extract was stored at (− 20 °C till use).

For this study, 40 male rats weighing 250–350 g of Wistar-Albino aged 10–12 weeks were obtained from the Inonu University Laboratory Animals Research Center and placed in a temperature (21 ± 2 °C) and humidity (60 ± 5%)-controlled room in which a 12:12-h light:dark cycle was maintained. The rats were fed a standard chow pellet diet and allowed free access to pelleted diet and drinking water. Randomization was used to assign animals to different experimental groups and to collect and process data, with analysis performed by investigators blinded to the treatment groups. The animals were maintained, and the experiments were performed in accordance with the Guidelines for Animal Research from the National Institutes of Health and the ARRIVE guidelines for reporting experiments involving animals [25]. The study protocol was approved by the Ethics Committee on Animal Research (ref. no: 2015/A-28) under the Faculty of Medicine, Inonu University, Malatya, Turkey. Simple randomization technique was used to allocate the rats to the groups for avoiding bias in the way the experiment was carried out. Forty male rats were randomly set into five groups ($n = 8$ for each group) as follows:

1. Control group: each rat in the group was treated with 1 ml of distilled water via orogastric gavage (o.g);
2. Acute low-dose group (ALD): 100 mg/kg of sPGe was dissolved in 1 ml of distilled water and applied via o.g for 1 day;
3. Subacute low-dose group (SALD): 100 mg/kg/day of sPGe was dissolved in 1 ml of distilled water and applied with o.g once a day for 28 days;
4. Acute high-dose group (AHD): 500 mg/kg of sPGe was dissolved in 1 ml of distilled water and applied with o.g for 1 day;
5. Subacute high-dose group (SAHD): 500 mg/kg/day of sPGe was dissolved in 1 ml of distilled water and applied with o.g once a day for 28 days.

Echocardiographic Analysis

At the end of the experiment, echocardiography (ECHO) was performed blindly under urethane anesthesia (1.5 mg/kg, intraperitoneally) to all the groups, as appropriate.

The animals were placed on controlled heating pads, and the core temperature was maintained at 37 °C. Transthoracic ECHO was performed in a supine position by a researcher who was blinded to the experimental groups after the anterior chest wall was shaved in all animals. Standard two-dimensional (2D) and M-mode long- and short-axis (at the midpapillary level) images were acquired using a 10-MHz linear transducer probe (GE parallel Design Inc. Phoenix, USA) with a commercially available ECHO system (Vivid 3; GE Healthcare, Phoenix, USA).

On M mode scanning of the parasternal long or short axis at the midpapillary level, interventricular septal thickness (IVSt) and left ventricle posterior wall thickness in diastole, as well as LV end-diastolic (LVED), and end-systolic diameter (LVES) were measured. End-systole was defined as the time point of minimal LV dimensions, whereas end-diastole was defined as the time point of maximal dimensions. Fractional shortening (FS) was determined from the measurements of LV chamber diameters: $FS = (LVED - LVES)/LVED \times 100$. LV volumes and ejection fraction (EF) were calculated according to the Teichholz formula [26]. LV filling was assessed by PW Doppler transmitral flow velocity tracings obtained just above the tip of the mitral leaflets. Peak early (E)- and late (A)-wave velocities, as well as E-wave deceleration time (EDT) were measured. Left atrial diameter (LA) and ascending aortic diameter (AA) were measured at parasternal long-axis view using 2D imaging. Three representative cardiac cycles were analyzed and averaged for each measurement. (See Supplementary Material Appendix 1).

Hemodynamic and Electrophysiological Analysis

Following the completion of the echocardiographic measurement, left carotid arteries of the rats were carefully cannulated, and systolic, diastolic, mean blood pressure (BP), and heart rate (HR) were monitored for 2 h. The data were used to evaluate acute and late-onset hemodynamic changes of sPGe administration in rats. Also, electrocardiographic (ECG) changes were recorded for 2 h using 3-lead ECG electrodes. ECG interpretations were performed in two ways: (1) by pattern evaluation and (2) by computerized reference. In brief, ECG data for (1) and (2) were evaluated visually at the end of the experiment by two professor

physicians (H.P. and N.E.) who were blind to the status and the groups of the animals. These physicians noted the electrophysiological variables and pathologic changes in the ECG trace including ST depression, T-wave negativity, QRS enlargement, QT prolongation, and atrioventricular block in the sPGe-administered groups. According to the Lambeth Convention criteria [27], both the arrhythmia diversity and the PR, QRS, and QT periods were calculated from the Biopac MP-100 Data Acquisition system (Biopac Systems, Inc., Santa Barbara, CA) (For details, see the Supplementary Material Appendix 2) [28]. All the rats were sacrificed after ketamine and xylazine (60 mg/kg and 6 mg/kg, i.p) administration. Then, blood samples from the inferior vena cava and the heart tissue were taken.

Histochemical Analysis

At the end of the experiment, heart tissues were fixed in 10% formaldehyde and were embedded in paraffin. 4–5-µm-thick sections were taken from the heart tissues. The sections were blindly stained with hematoxylin–eosin (H–E) staining to determine the general morphological structure and orcein for determining the elastic lamella. General morphologic parameters for heart tissues include congestion–hemorrhage, infiltration, interstitial edema, and cardiomyocyte degeneration (dense eosinophilic cytoplasm and pyknotic nucleus). For semiquantitative scoring of each variable, the following scale was used: 0, normal tissue; 1, damage involving < 25% of the total area; 2, damage involving 25–50% of the total area; 3, damage involving > 50% of the total area. Histopathologic evaluations were performed using a Leica DFC280 light microscope and a Leica Q Win Image Analysis system (Leica Micros Imaging Solutions Ltd., Cambridge, UK) [29].

Immunohistological Method and Analysis

4-µm-thick tissue sections were deparaffinized, rehydrated, and placed in antigen retrieval solution (citrate buffer, pH 6.0), and boiled in a pressure cooker for 20 min and cooled to room temperature for 20 min. Then, the sections were washed with phosphate-buffered saline (PBS, pH 7.4) and, for blocking endogenous peroxidase activity, the slides were incubated in 0.3% hydrogen peroxide solution for 15 min at room temperature and then washed in PBS. After the blocking of non-specific antigen-binding sites with protein block, caspase-9 (Thermo Fisher Scientific, CA, USA, Rabbit Polyclonal Antibody, Catalogue Number: RB-1205-P0, Lot No: 1312A, Epitope: aa 1-134, isotype: IgG, Clone Number: LAP6 Ab-4) and desmin (Santa Cruz Biotechnology, CA, USA, Mouse Monoclonal Antibody, Catalogue Number: sc-23879, Lot No: H1016, Epitope: N/A, isotype: IgG, Clone Number: N/A) were applied for 60 min at room temperature. After being rinsed with PBS, the sections were incubated with biotinylated secondary antibody and streptavidin-peroxidase for 10 min at room temperature. The samples were blindly visualized with the chromogenic substrates AEC, counterstained with hematoxylin, and mounted on a glass slide.

Histochemical and immunohistological examinations were performed by two histologists (N.V. and A.Y.) who were blind to the status and groups of animals. The mean values were used in the result section, as appropriate.

According to the prevalence of the staining, the sections were graded as 1 = 0–25% staining; 2 = 25–50% staining; 3 = staining 51–75%; 4 = staining 76–100%. According to the staining intensity, the sections were graded as follows: 0 = no staining; 1 = weak but detectable staining; 2 = distinct; 3 = intense staining. Total staining score was obtained as (prevalence)X(intensity) [30].

Terminal Transferase-Mediated dUTP Nick End-Labeling (TUNEL) Method and Analysis

5–6-µm cross sections obtained from paraffin blocks were transferred to polylysine glass slides. ApopTag Plus Peroxidase In Situ Apoptosis Detection Kit (Chemicon, Cat. No: S7101, USA) was used in a manner conforming to the directions of the manufacturer for determining the cells that underwent apoptosis. The rat breast tissue was used as the positive control, whereas a Reaction Buffer was used instead of the prepared solution as the negative control.

Tissues that were deparaffinized via xylene were passed through graded alcohol series and washed with phosphate-buffered saline (PBS). The tissues that were incubated for 10 min via 0.05% proteinase K were then incubated for 5 min via 3% hydrogen peroxide in order to prevent endogenous peroxidase activity. The tissues were incubated using equilibration buffer for 6 min after being washed with PBS after which they were subject to incubation for 60 min at 37 °C in a humid working environment via working solution (70% µl reaction buffer + 30% Terminal deoxynucleotidyl transferase enzyme). The tissues were left to wait in stop/wash buffer for 10 min after which they were handled for 30 min via anti-digoxigenin-peroxidase. Apoptotic cells were imaged via diaminobenzidine (DAB) substrate. The cross sections were counterstained via Harris hematoxylin after which they were locked using a proper locking solution. The preparations were examined, evaluated, and photographed via Novel N-800M microscope. The nuclei dyed blue via Harris hematoxylin for the evaluation of the TUNEL staining along with the nuclei with normal brown nuclear staining was evaluated apoptotically. A minimum of 500 cells was counted as normal and apoptotic in the randomly selected areas on the 10 times magnified cross sections. Apoptotic index (AI) was calculated, and statistical

analyses were made with the proportioning of the apoptotic cells to the total number of cells.

Real-Time Quantitative Polymerase Chain Reaction (RT-qPCR)

The heart samples were stored in 1 ml of RNA-later solution at − 86 °C until the examination were carried out. Total RNA isolation was performed from rat heart tissue with High Pure RNA Tissue Kit (Roche Lot No: 11596700, Ref. No: 12033674001). Total RNA was run on 1% agarose gel and the degradation of the mRNA was blindly inspected by visualization of ribosomal bands with ethidium bromide over a UV transilluminator. The concentrations of the purified RNA were determined by a spectrophotometer (Biotek, Epoch). Transcriptor First-strand cDNA Synthesis Kit (Roche, Lot No: 11260125, Ref. No: 04 896 866 001) was used for reverse transcription (RT) reactions, and the manufacturer's suggested protocol was applied. Oligo (dT)-18 primer and random hexamer primers were mixed in the same reaction and used to extend all mRNA, and equal amounts of total RNA were added to each reverse transcription reaction. Quantitative PCR (qPCR) was carried out using Fast Start Essential DNA Probes Master Kit (Roche Lot No: 11806100, Ref. No: 06 402 682 001) and real-time ready assays *β-Actin*, (Ref. No: 05532957001 Lot No: 0000010971, Assay ID: 500152, Config. No: 100081783); *Cu/Zn-SOD1* (*copper/zinc-superoxide dismutase*), (Ref. No: 05532957001, Lot No: 0000010972, Assay ID: 503225, Config. No: 100081774); *CAV1* (*Caveolin-1*), (Ref. No: 05532957001, Lot No: 0000010973, Assay ID: 500576, Config. No: 100086894), *VEGF-A* (*Vascular endothelial growth factor*) (Ref. No: 05532957001, Lot No: 0000010974, Assay ID: 500471, Config. No: 100072226) (Table 1) with Real-Time PCR instrument (Roche LC96). The PCR mixture contained 2.5 µl of cDNA, 2 µl PCR grade water, 0.5 µl of real-time ready assay mix hydrolysis probe, and primers, and 5 µl of Fast Start Essential DNA Probes Master kit. Amplification was performed at 95 °C for 10 min, followed by 55 cycles of 95 °C for 10-s denaturation, 60 °C for 30-sec annealing, and 72 °C for 1-s extension. All qPCR applications were performed in three replicates in the same plate including the housekeeping gene. After the amplification, PCR products were run in 2% agarose gels, and single and appropriate size DNA bands were obtained for *β-Actin, Cu/Zn-SOD1, CAV1*, and *VEGF-A* (Fig. 1a, b). Relative mRNA expression levels of *Cu/Zn-SOD1, CAV1*, and *VEGF-A* were calculated based on the *β-Actin* housekeeping gene using the $2^{-\Delta\Delta}$Ct method [31].

Biochemical Studies

The blood samples of the rats were centrifuged at 3500 rpm for 7 min. The serum samples were taken into Eppendorf tubes and stored in the refrigerator (− 86 °C) in Inonu University Biotechnology Research and Application Unit. One day prior to biochemical analysis, frozen samples were moved to a + 4 °C unit to dissolve. Then, serum blood urea nitrogen (BUN), creatinine (Cr), cholesterol, high-density lipoprotein (HDL), low-density lipoprotein (LDL), creatine kinase (CK), sodium, potassium, pro b-type natriuretic peptide (pro-BNP), troponin-I, and myoglobin parameters were studied in Turgut Ozal Medical Center Laboratories, Inonu University, Malatya, Turkey.

Materials

Standardized *Panax ginseng* C.A. Meyer dry extract HRS (Product code: Y0001029, EDQM, Strasbourg, France), the main intervention and urethane (Acros Organics, Product code: 325540500, New Jersey, USA) an irreversible anesthetic agent were purchased from Sigma–Aldrich Chemical. Ketamine (Alfamine®) and Xylazine (Alfazyne®) were from Ata-fen Company, Izmir, Turkey. Primer antibodies (ki-67 antibody) were from Thermo Fisher Scientific, UK. Further detail of genetic materials can be found in the RT-qPCR section of the "Methods" part.

Data Analysis

The data and statistical analysis comply with the recommendations on experimental design and analysis in

Table 1 Primer sequences for housekeeping and target genes

Genes	Primer sequence (5′–3′)	NCBI reference sequence	Amplicon length (bp)
β-Actin	F: 5′ CTAAGGCCAACCGTGAAAAG 3′ R: 5′ GCCTGGATGGCTACGTACA 3′	NM_031144.3	79
CAV1	F: 5′AACGACGACGTGGTCAAGAT 3′ R: 5′CACAGTGAAGGTGGTGAAGC 3′	NM_031556.3 NM_133651.2	105
Cu/Zn-SOD1	F: 5′ GGTCCAGCGGATGAAGAG 3′ R: 5′ GGACACATTGGCCACACC 3′	NM_017050.1	78
VEGF-A	F: 5′AAAAACGAAAGCGCAAGAAA 3′ R: 5′TTTCTCCGCTCTGAACAAGG 3′	NM_001110335.1	73

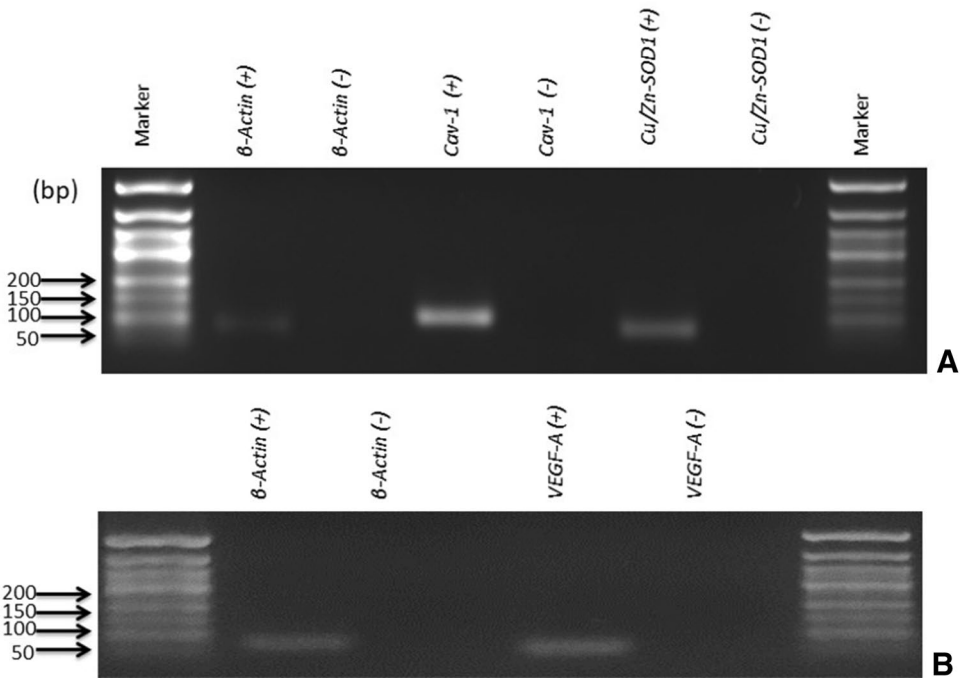

Fig. 1 Agarose gel electrophoresis RT-qPCR results of β-actin, Cav-1, Cu/Zn-SOD1 (**a**) and VEGF-A (**b**) mRNA. The products were loaded on 2% DNA agarose gel, and the size of each mRNA was determined by a DNA marker (Bioron, 50 bp, catalog no: 304007). PCR conditions and expected size of PCR products are given in "Methods" section. mRNA was not loaded in the negative lanes to indicate the absence of primer dimers

pharmacology [32]. For detecting even minor effects, the required power and sample sizes used in this experiment were identified using the statistical power analysis. Sample size estimates for in vivo studies are based on a survey of data from published research and preliminary studies. To detect a twofold change between experimental groups, power analysis—using probability of type I error $\alpha = 0.05$; probability of type II error $\beta = 0.20$, along with previous laboratory data,—indicated that the minimum sample size required to detect a significant difference of HR values of pilot study should be at least $n = 8$ per group (40 in total) in each experiment group using the Web-Based Sample Size & Power Analysis Software [33]. The normality of the distribution of the data was evaluated through the Kolmogorov–Smirnov Z test. According to the results obtained from the normality test, Kruskal–Wallis H test was used for comparing the groups with respect to gene expression and echocardiographic data. Then, Conover's test was used in multiple comparisons of echocardiographic, electrocardiographic, immunohistochemical, and genetic data between the groups, as appropriate. Intragroup comparisons of the hemodynamic data were performed by the Friedman test, and multiple comparisons were carried out using the Bonferroni adjusted Wilcoxon test. The values of "p" which are less than 0.05 were considered statistically significant. IBM SPSS Statistics v. 24 SPSS Inc., Chicago, IL for Windows package program was used for the data analysis.

Results

Body Weight–Experimental Toxicity

No animals deceased during or after the sPGe administration or surgical procedures. Both acute and subacute sPGe administration promoted weight gain in the rats. However, there was just a significant difference in SAHD group compared to the control group (data not shown).

ECG Results

The results are shown in Table 2 and Supplementary Material Appendix 3. In this study, 2 out of 8 rats in SALD group were affected with AV blocks. In addition, ST depression was seen on 3 out of 8 rats in ALD group, whereas T negativity was observed on 2, 2, and 3 rats in ALD, AHD, and SAHD groups, *respectively*. In terms of electrophysiological parameters, QT interval tended to increase but not significantly in SAHD group.

Effects on the Cardiohemodynamic Parameters

The cardiohemodynamic variables were measured at the final stage of the experiment ($n = 8$). The time courses of changes in the HR, systolic, diastolic, and mean arterial

Table 2 ECG findings and incidence of cardiac rhythm disorders

Groups ($n=8$)	PR interval (ms)	QRS width (ms)	QT interval (ms)	ST depression	AV block	T negativity
Control	44 (26–52)	68 (58–80)	100 (92–108)	–	–	–
Acute low dose	38 (32–48)	69 (44–86)	106 (96–116)	3	–	2
Subacute low dose	44 (30–54)	75 (66–100)	113 (98–130)	–	2	–
Acute high dose	42 (36–58)	74 (48–100)	108 (84–122)	–	1	2
Subacute high dose	42 (36–44)	75 (60–84)	123 (104–168)	–	1	3

Values are median (min–max). Values at ST depression, AV block, and T negativity columns indicate the number of affected rats in the particular group

Table 3 Acute and late-onset changes in the heart rate, systolic blood pressure, diastolic blood pressure, and mean blood pressure at the end of the experiment

Groups	Variables	0 min	10 min	30 min	60 min	90 min	120 min
Control	Heart rate (beats/min)	393 (230–513)	370 (240–512)	324 (245–512)	337 (220–513)	299 (245–513)	315 (260–513)
Acute low dose		353 (254–440)	346 (267–420)	330 (264–414)	342 (268–410)[e,f]	382 (333–530)[a,c]	374 (344–510)[a,c]
Subacute low dose		300 (260–336)	303 (260–344)[d,f]	309 (288–370)[f]	349 (310–400)[a]	342 (300–410)	377 (340–434)[a]
Acute high dose		338 (294–462)	335 (248–518)	344 (226–473)	366 (242–475)	354 (241–428)	361 (258–428)
Subacute high dose		326 (205–385)	326 (200–384)	326 (230–357)	304 (230–360)	355 (330–389)	368 (332–394)
Control	Systolic blood pressure (mmHg)	111 (72–149)	107 (73–118)	89 (69–137)	89 (71–156)	88 (70–154)	90 (69–137)
Acute low dose		114 (75–143)	118 (65–142)	99 (74–155)	111 (72–157)	122 (95–156)	125 (40–153)
Subacute low dose		106 (75–134)	101 (57–131)	98 (56–110)	100 (58–119)	101 (53–128)	102 (67–119)
Acute high dose		118 (84–144)	114 (91–132)	101 (69–136)	100 (58–175)	111 (67–139)	118 (76–141)
Subacute high dose		99 (87–145)	90 (82–148)	86 (66–124)	91 (67–114)	92 (73–119)	99 (69–123)
Control	Diastolic blood pressure (mmHg)	62 (33–97)	48 (36–90)	54 (32–82)	63 (28–75)	65 (23–75)	72 (40–80)
Acute low dose		52 (30–61)	47 (37–84)	42 (34–72)	44 (25–70)	48 (31–72)	44 (27–72)[1]
Subacute low dose		40 (10–68)	45 (25–55)	43 (29–60)	48 (30–55)	47 (26–61)	53,5(42–63)[1]
Acute high dose		52 (29–82)	51 (28–106)	45 (25–101)	49 (33–97)	52 (28–95)	58(31–104)[2]
Subacute high dose		45 (25–63)	47 (20–63)	37 (23–45)	37 (23–68)	53 (28–68)	51(34–65)
Control	Mean arterial blood pressure (mmHg)	84 (65–110)	79 (67–102)	78 (71–92)	81 (67–104)	72 (44–103)	85 (74–100)
Acute low dose		72 (52–82)	69 (53–85)	65(52–74)[a,1]	68 (43–76)[d,1]	74 (52–87)[c]	69 (32–87)[1]
Subacute low dose		65 (52–95)	68 (48–88)	63 (50–73)[a,1]	69 (53–80)	61 (48–86)[a]	73 (65–82)[1]
Acute high dose		78 (54–88)	72 (53–111)	63 (39–107)[1]	63 (48–100)[1]	76 (41–108)[a,b,c]	83 (47–105)
Subacute high dose		65 (45–89)	65 (37–89)	53 (37–69)[b,1,3]	54 (47–75)[1]	68 (50–74)[b]	65 (56–81)[1,3]

Data are expressed as median (min–max). $n=8$ for each group

[a]p<0.05: Significant compared to 0 min in the same row

[b]p<0.05: Significant compared to 10 min in the same row

[c]$p < 0.05$: Significant compared to 30 min in the same row

[d]$p < 0.05$: Significant compared to 60 min in the same row

[e]$p < 0.05$: Significant compared to 90 min in the same row

[f]$p < 0.05$: Significant compared to 120 min in the same row

[1]$p < 0.05$: Significant compared to control group for the same parameter

[2]$p < 0.05$: Significant compared to acute low-dose group for the same parameter,

[3]$p < 0.05$: Significant compared to acute high-dose group for the same parameter,

BP are summarized in Table 3. During 2 h of observation, there were no significant changes in hemodynamic variables in control group compared to the pre-drug (0 min) values in the same group ($p > 0.05$). In terms of HR, there were significant increases at the 90 and 120 min at the ALD group, and there were also statistically significant increases at the 60 and 120 min at the SALD group compared to their pre-drug control values, *respectively*. There was no statistically significant difference in systolic BP data during monitorization. But, there was a decreasing pattern till 30 min in ALD and SAHD groups compared to the pre-drug value of diastolic BP. Significant decreases were detected in the mean arterial BP for 30 min in ALD and SALD groups ($p < 0.05$), and for 90 min in SALD and AHD groups ($p < 0.05$) compared to the pre-drug value (For the pattern of changes during observation, see the Supplementary Material Appendix 4). There were no significant changes in high dose of sPGe-administered groups in terms of systolic, diastolic, mean arterial BP, or HR.

Mean BP values at 30, 60, and 120 min were significantly higher in control group as compared to ALD and SAHD groups ($p < 0.05$). Mean BP in AHD group at 30 and 60 min and in SALD group at 30 and 120 min were lower than the control group ($p < 0.05$). Diastolic BP was significantly decreased in low-dose sPGe-applied groups compared to control group ($p < 0.05$).

Effects on the Variable of the ECHO

Typical recordings of flow velocity pattern and tissue Doppler imaging are shown in Supplementary Material Appendix 1, and the effects of sPGe on the variables of ECHO are summarized in Table 4. sPGe decreased the peak velocity of E/A-wave in all sPGe-applied groups compared to control group ($p < 0.05$). LVES and LVED tended to increase in the all sPGe-administered groups; besides the neutral effect of sPGe on cardiac diameters and systolic functions, there was substantial diastolic left ventricle filling wave velocity alteration in all sPGe-administered groups compared to the control group ($p < 0.05$). But sPGe application did not alter AA, IVSt, EF, FS, and EDT variables among groups ($p > 0.05$).

Laboratory Analysis

The blood parameters are summarized in Table 5. When the groups were compared in terms of the BUN, Cr, cholesterol, HDL, LDL, CK, sodium, potassium, pro-BNP, troponin-I, and myoglobin variables, only LDL, sodium, troponin-I, and myoglobin variables were statistically significant ($p < 0.05$). LDL and troponin-I tended to increase except ALD group; however, LDL, troponin-I, and myoglobin levels in ALD group and LDL in SAHD group were significantly lower than AHD group. Acute high-dose sPGe injection caused statistically significant elevation on myoglobin marker in AHD group compared with control group. Also, there was a statistically, however not clinically significance on sodium

Table 4 The effects of sPGe administration on the variables of the echocardiography in rats

Variables	Control	Acute low dose	Subacute low dose	Acute high dose	Subacute high dose
AA (mm)	3.1 (2.8–3.5)	2.9 (2.5–3.2)	2.9 (2.7–3.6)	3.3 (2.4–4)	2.9 (2.2–3.3)
LA (mm)	3.9 (2.9–4.8)	3.8 (3–4.1)[b]	4.1 (3.2–4.5)[a]	4.7 (3.6–5.3)[c]	4 (3.2–4.7)
IVSt (mm)	2 (2–2)	2 (1–2)	2 (2–2)	2 (2–3)	2 (1–3)
LVES (mm)	2 (1–4)	4 (1–4)[a]	4 (2–4)[a]	3 (2–4)	3 (2–5)
LVED (mm)	5 (5–7)	6 (4–6)	6 (5–7)	6 (5–6)	6 (4–7)
EF (%)	95 (76–99)	75 (67–97)	83 (74–92)	83 (71–92)	81 (53–93)
FS (%)	64 (40–78)	39 (32–71)	47 (38–58)	47 (36–59)	47 (23–60)
E-wave	0.85 (0.74–0.97)	0.66 (0.4–0.84)[a]	0.66 (0.56–0.9)[a]	0.63 (0.3–0.71)[a]	0.64 (0.5–0.93)[a]
A-wave	0.26 (0.15–0.52)	0.24 (0.18–0.64)	0.41 (0.24–0.82)	0.33 (0.21–0.52)	0.44 (0.14–0.84)
E/A	3.6 (1.4–6)	2.9 (0.7–3.6)[a]	1.8 (0.8–3.1)[a]	2.1 (0.7–3.2)[a]	2.4 (0.7–4.3)[a]
EDT (ms)	30 (26–37)	33 (18–48)	35 (18–55)	36 (18–55)	26 (15–48)

Data are median (min–max). $n = 8$ for each group

AA ascending aortic diameter, *LA* left atrial diameter, *IVSt* interventricular septal thickness in diastole, *LVED* left ventricular end-diastolic diameter, *LVES* left ventricular end-systolic diameter, *EF* ejection fraction, *FS* fractional shortening, *E/A* peak velocity of E-wave/peak velocity of A-wave, *EDT* E-wave deceleration time

[a]Versus control group ($p < 0.05$)

[b]Versus acute high-dose group

[c]Versus subacute high-dose group

Table 5 Blood chemistry parameters at the end of the experiments in the all groups

Variables	Control	Acute low dose	Subacute low dose	Acute high dose	Subacute high dose
BUN (mg/dL)	36 (28–69)	52 (36–61)	46 (40–66)	41 (26–62)	49 (26–69)
Cr (mg/dL)	1 (1–1)	1 (1–1)	1 (1–1)	1 (0–1)	1 (1–1)
Cholesterol (mg/dL)	52 (39–58)	46 (34–67)	51 (43–61)	47 (38–53)	49 (36–62)
HDL (mg/dL)	28 (24–33)	24 (19–35)	28 (11–33)	25 (23–26)	27 (17–32)
LDL (mg/dL)	9 (2–21)	4 (2–7)	10 (3–18)	14 (10–16)	7 (1–10)
CK (U/L)	1633 (967–3400)	2712 (971–4267)	2610 (1203–4267)	1520 (1181–4267)	2575 (1050–4267)
Sodium (mmol/L)	145 (139–151)	139 (133–146)	139 (137–143)	140 (135–145)	139 (134–144)[a]
Potassium (mmol/L)	6 (5–7)	7 (5–7)	6 (5–10)	7 (6–8)	7 (6–10)
Pro-BNP (pg/mL)	20 (20–20)	23 (20–60)	21 (20–51)	20 (20–26)	20 (20–26)
Troponin I	8539 (938–19,586)	6300 (1547–10,928)	17,073 (1360–50,001)	18,785 (10,610–48,436)	18,825 (5438–41,310)
Myoglobin	298 (85–602)	299 (171–744)[c]	509 (158–1201)	802 (483–1201)[a]	684 (374–1166)

Data are median (min–max). $n = 8$ for each group

BUN blood urea nitrogen, *Cr* creatinine, *HDL* high-density lipoprotein, *LDL* low-density lipoprotein, *CK* creatine kinase, *pro-BNP* pro b-type natriuretic peptide

[a] $p < 0.05$: Significant compared to control group in the same row

[b] $p < 0.05$: Significant compared to acute low-dose group in the same row

[c] $p < 0.05$: Significant compared to acute high-dose group in the same row

levels between control and SAHD groups. No significant differences were detected in the other parameters.

Immunohistochemical Analysis

General Morphology of the Myocardial Tissue

In the general morphological evaluation of myocardium, congestion–hemorrhage, infiltration, interstitial edema, and degenerated cardiomyocyte were examined. In the control group, heart tissue was in normal histological appearance except for mild changes (Fig. 2). ALD and SALD groups were statistically similar to the control group ($p > 0.05$) (Table 6), in terms of all mentioned parameters. However, compared to all groups, the severity of interstitial edema increased significantly in AHD group ($p < 0.05$). In addition, degenerated cardiomyocytes were found to be statistically more intense in the AHD and SAHD groups ($p < 0.05$) (Fig. 2; Table 6).

Desmin Immunoreactivity Scores

Desmin immunoreactivity was significantly observed in Z disks and intercalated disks (Fig. 2). The highest expression among the groups was observed in the control group, while the lowest expression was observed in the AHD group. Also, there was no statistically significant difference between ALD and SALD groups. Immunoreactive desmin score of AHD group was significantly lower than that of SAHD group ($p < 0.05$). The positive control was heart tissue for desmin antibody, whereas negative control was not used in the experiment.

Caspase-9 Immunoreactivity Scores

The caspase-9 immunoreactivity observed in the cytoplasm of cardiomyocytes (Fig. 2) was not significant among the groups ($p > 0.05$). The highest immunoreactivity was observed in AHD group. Compared with the control group, elevation in AHD group was found as statistically significant ($p < 0.05$). In addition, there was no difference between ALD and SALD groups ($p > 0.05$). Caspase-9 immunoreactivity of SAHD group was significantly lower than that of AHD group ($p < 0.05$). The positive control was tonsil for the caspase-9 antibody.

TUNEL Results

TUNEL positivity in the heart tissue was similar between control and ALD groups ($p > 0.05$). TUNEL positive cells were mostly observed in the SALD group. Compared with control group, there was a significant increase in SALD group ($p < 0.05$). Also, a statistically significant decrease was observed in the AHD and SAHD groups compared with° SALD group ($p < 0.05$) (Fig. 2).

Results of Gene Expressions

In the current study, the data of the gene expressions of *Cu/Zn-SOD1, VEGF-A*, and *CAV1* in heart tissue of the different treatment groups are summarized in Table 7. Briefly,

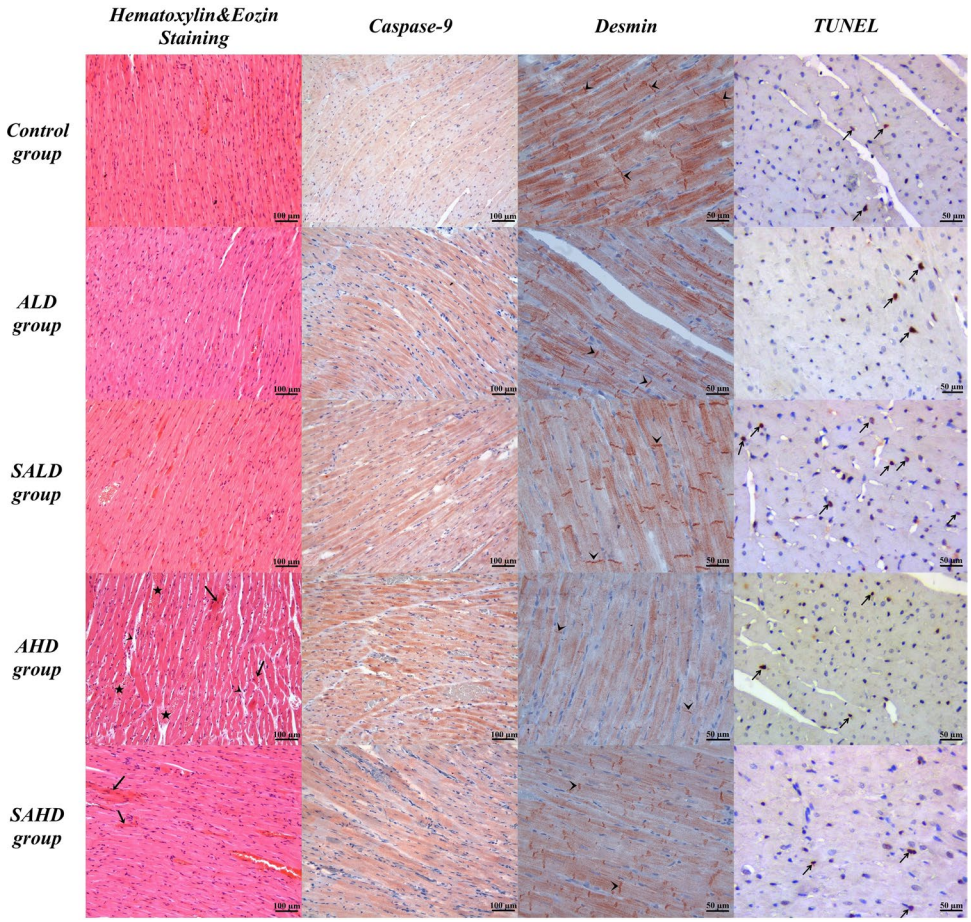

Fig. 2 Immunohistochemical appearance of heart tissue. Hematoxylin and eozin staining: control: normal histological appearance of myocardial tissue. ALD group and SALD group: the appearance of the myocardial tissue is similar to the control group. AHD group: congestion (stars), intestinal edema (arrowheads), and degenerated cardiomyocytes (arrows). SAHD group: degenerated cardiomyocytes (arrows). H–E: ×20. Desmin activity: Banded pattern of staining on myofibrils on longitudinal section (arrowheads) intercalated disks are clearly visible, ×40. Caspase-9: Caspase-9 immunoreactivity in the cytoplasm of cardiomyocytes, ×40. TUNEL: Arrows indicate TUNEL positive cells, ×40

Table 6 Semiquantitative scores of infiltration, congestion-hemorrhage, interstitial edema, degenerative cardiomyocytes, and immunoreactive scores of desmin, caspase-9, and percentage of apoptotic index of the myocardium

Groups ($n=8$)	Infiltration	Congestion–hemorrhage	Interstitial edema	Degenerative cardiomyocytes	Desmin	Caspase-9	Apoptotic Index (%)
Control	0 (0–2)	1 (0–2)	0 (0–2)	0 (0–2)	6 (1–12)	2 (0–8)	3
Acute low dose	0 (0–2)	1 (0–3)	0 (0–3)	0 (0–3)[a]	4 (1–12)[a,d]	2 (0–12)[d]	3
Subacute low dose	0 (0–2)	1 (0–3)	0 (0–2)	0 (0–3)[a]	4 (1–12)	2 (0–8)	12[a]
Acute high dose	0 (0–1)	1 (0–3)[a]	0 (0–3)[a,b]	0 (0–3)[a]	2 (0–9)[a,e]	3 (0–12)[a]	3[c]
Subacute high dose	0 (0–3)	1 (0–3)	0 (0–2)[d]	1 (0–3)[a,c]	4 (1–12)	2 (0–9)[d]	4[c]

Data are presented as median (min–max)

[a] $p < 0.05$: Significant compared to control group in the same column

[b] $p < 0.05$: Significant compared to acute low-dose group in the same column

[c] $p < 0.05$: Significant compared to subacute low-dose group in the same column

[d] $p < 0.05$: Significant compared to acute high-dose group in the same column

[e] $p < 0.05$: Significant compared to subacute high-dose group in the same column

these results showed that increasing the dose and duration caused a highly significant increase in the gene expression of *Cu/Zn-SOD1,* but did not affect the *VEGF-A* and *CAV1* genes in the sPGe-administered groups compared with the control group.

Discussion

Ginseng, also referred to by its genus name *Panax*, stemming from *panacea* derived from the Greek goddess of

Table 7 Changes of gene expressions in the heart tissue

Groups ($n=8$)	Cu/Zn-SOD1	VEGF-A	CAV1
Control	41.38 (26.19–70.52)[b,c,d,e]	12.5 (3.3–22.8)	13.29 (5.07–52.75)
Acute low dose	72.05 (33.02–204.73)[a,c,d,e]	14.9 (4.5–41.3)	17.28 (5.36–19.29)
Subacute low dose	257.77 (72.63–1305)[a,b,d,e]	14.1 (9.1–61.9)	14.76 (4.27–28.32)
Acute high dose	1365.33 (696.27–3152.67)[a,b,c,e]	14.9 (7.6–21)	25.04 (8.28–59.21)
Subacute high dose	5820.66 (2266.33–11319)[a,b,c,d]	20.7 (7.2–47.9)	31.73 (14.81–70.20)

Data are expressed as median (min–max)

Cu/Zn-SOD1 Copper–zinc superoxide dismutase, *VEGF-A* vascular endothelial growth factor A, *CAV1* caveolin 1

[a]p <0.05: Significant compared to control group in the same column

[b]p <0.05: Significant compared to acute low-dose group in the same column

[c]p <0.05: Significant compared to subacute low-dose group in the same column

[d]p <0.05: Significant compared to acute high-dose group in the same column

[e]p <0.05: Significant compared to subacute high-dose group in the same column

healing, was considered to be due to the close resemblance of the ginseng root [34]. Many pieces of researches have focused on individual ginsenosides instead of the whole ginseng against many disease conditions [35–37].

Contrary to what we have expected based on previously reported cardiac effects of *Panax ginseng* [38–40]; in the present study, we found that sPGe might cause myocardial damage and also triggered a pathophysiology of diastolic heart failure without effecting ejection fraction in a dose and duration-dependent use. However, we did not notice any significant effects on left ventricular systolic functions, HR, BP nor any electrophysiological variables on ECG. However, we determined a trend in reduction in BP and prolonged QT interval which did not reach a statistically significant value. However, our study protocol did not include any pathological conditions, such as hypertension, ischemic heart disease, or cardiac arrhythmia, for which a variety of ginseng family and ginsenosides were already tested, mostly producing promising effects [41–43].

In the ECG analyses, ST depression, T-wave negativity, and AV blocks were observed in the sPGe-administered groups. We did not notice statistically significant effects on electrophysiological parameters in terms of PR interval showing AV node transmission and QRS duration, which showed intraventricular conduction. In addition, QT interval tended to increase, but not significantly in SAHD group, but might be clinically important [14]. However, Ginsenoside Re which is found in both various ginseng forms was shown to reduce HR, shorten the plateau phase of action potentials, and decrease P-wave amplitude, indicating blockade of slow Ca^{2+} channels mainly in the atria [44]. Caron et al. found that *Panax ginseng*, at doses of 200 mg of the extract daily, prolonged the QTc interval and decreases diastolic BP 2 h after ingestion in healthy adults on the first day of therapy [6]. Moreover, Jiang and colleagues reported that *Panax quinquefolius* use in rats resulted in significant PR, QRS, and QT prolongation with reduced ventricular force generation and BP [45].

According to the echocardiographic examination, we did not notice the negative or positive effects of sPGe on the contractility and diameter of rat hearts including left atrium and ascending aorta. Jiang et al. reported the negative inotropic effect of *North American ginseng* which has a different kind of ginsenoside profile [45]. In that study, reduced contractility explained as decreased intracellular Ca^{2+} transient changes, shown by using the fluorescent indicator fura-2 in freshly isolated cardiac myocytes. In another study, *Shenfu* formula used in traditional Chinese medicine containing *Panax ginseng*, tested in ischemic heart failure model and resulted with increased the left ventricular EF, improved the hemodynamic index of heart failure rats, and decreased serum BNP levels [43]. Although we did not observe the impact on cardiac systolic functions, there is a substantial alteration in diastolic left ventricle filling wave characteristics. We do not know the exact mechanism(s) underlying this alteration, but we can say that this is the first study that shows sPGe may trigger diastolic dysfunction in the heart without effect the EF.

As an important finding, diastolic BP tended to decrease after sPGe administration till 30 min, whereas HR values showed an increasing pattern after 30 min in the ALD and SALD groups. First, the sPGe decreased the diastolic BP, and then the body started to increase HR which was defined as reflex tachycardia, to compensate for this situation. As seen, diastolic BP and HR values in ALD and SALD groups were 42 mmHg, 330 beats/min and 43 mmHg, 309 beats/min at 30 min, whereas they were 48 mmHg, 382 beats/min in 90 min and 54 mmHg and 377 beats/min at 120 min, *respectively*. When we reevaluated this original finding with the recently published liquid chromatography report of sPGe (Fig. 3), ginsenoside Rb1, Rb2, and Rc ingredients reached the highest concentration

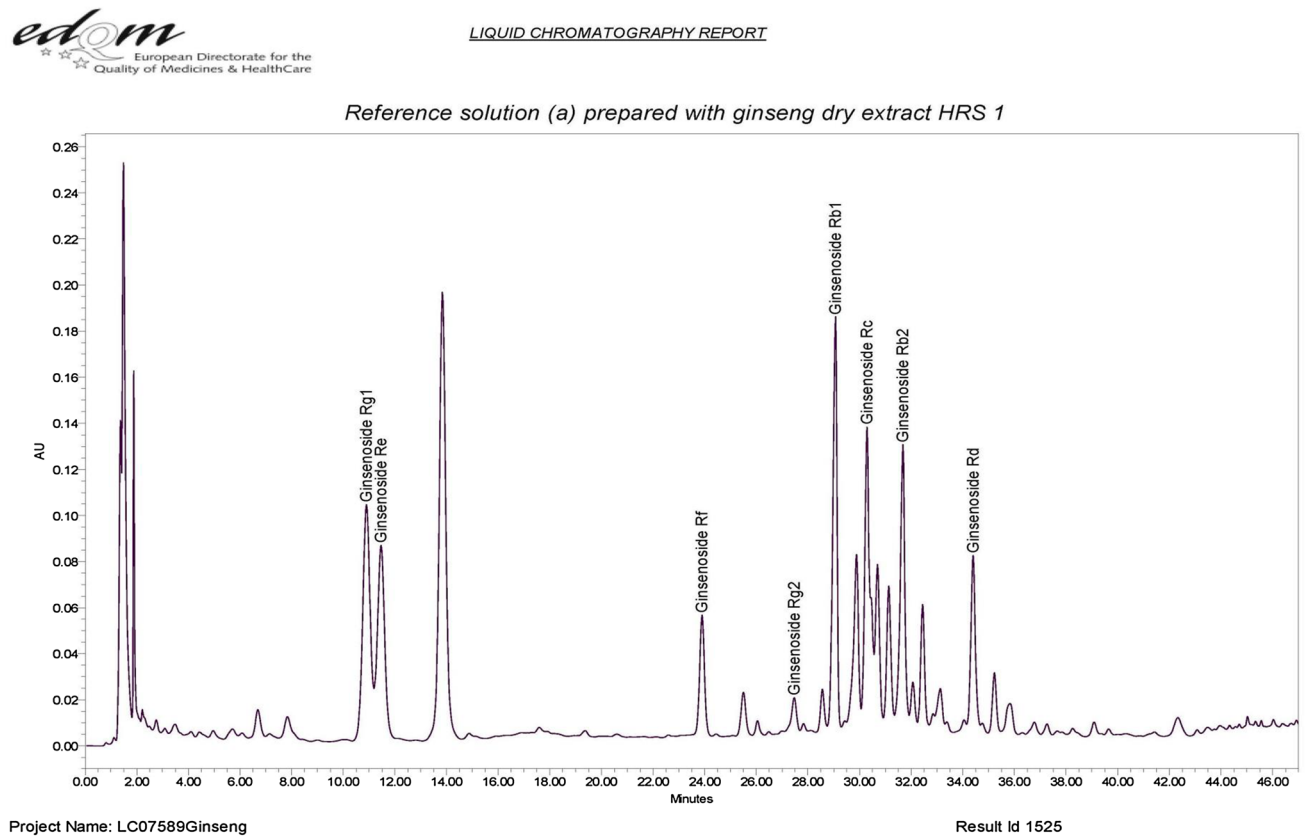

Fig. 3 Liquid chromatography report for sPGe (ginseng dry extract HRS). See Information leaflet of Ph. Eur. Reference Standard of Ginseng Dry Extract HRS (Catalogue Code: Y0001029, *European Directorate for the Quality of Medicines & HealthCare*, European Pharmacopoeia (Ph. Eur.) 7, Allée Kastner CS 30026, F-67,081 Strasbourg (France). Last Access Date: 15/02/2019

in the blood at about 30 min after sPGe administration, whereas ginsenoside Re and Rg1 ingredients reached the highest concentrations at about 10–12 min. *Panax ginseng* demonstrated various pharmacological activities by regulating many mechanisms of action due to the active ingredients. Another study showed that ginsenoside Re activates potassium channels of vascular smooth muscle cells through phosphoinositide-3-kinase–protein kinase ß-actin and NO pathways [46].

Prior preclinic studies although have suggested that ginseng has direct vasodilatory and BP reducing effects through the generation of endothelium-dependent NO and subsequent cyclic guanosine monophosphate [10, 41] in humans, a systematic review and meta-analysis of 17 randomized control trials in 1381 individuals with and without hypertension, resulted with an overall neutral effect of ginseng on systolic, diastolic and mean BP, compared with control group [47]. Related to the HR issue, some of the prior the preclinical studies parallel to human studies reported a negative chronotropic effect of ginseng family [44, 48], which might aid in reducing BP and control ischemia in coronary artery disease.

The echocardiographic evaluations after the study did not show any significant changes in functional parameters such as left ventricular diastolic–systolic diameters, wall thicknesses, EF, and FS by sPGe at different doses and application durations. Although cardiac troponin I, which indicates cardiac damage, tended to increase in the all groups except for ALD group; this suggested that a left ventricular systolic function, which could be detected by ECHO, was not at a level that can cause change. However, the change in the parameters that indicate the diastolic function of the left ventricle was noteworthy. Mitral E-wave velocity corresponding to an early filling of the left ventricle was reduced after sPGe uses except for the ALD group. We also found that A-wave, which related a mitral late filling, increased in groups where sPGe was used for a long time. The changes in mitral E- and A-wave velocities and E/A ratio indicated that diastolic functions might be affected by sPGe use, which implied an increased risk for preserved EF heart failure [49, 50]. This finding suggests that sPGe has the potential to cause cardiac injury depending on the dose and duration of use, suggesting that patients should be carefully monitored and warned of heart damage when using this agent. There were no significant differences among the groups related

to other biochemical parameters, including lipid profile, which is a risk for atherosclerosis.

Acidophilic cytoplasm and pycnotic nucleus in myocardial fibers were observed in AHD and SAHD groups. The formation of eosinophilic cells associated with a decrease in intracellular pH level reported in doxorubicin-induced cardiotoxicity [51] and myocardial ischemia–reperfusion model [52, 53]. The increase of intracellular acidosis activated various enzymes such as RNAase. Activated enzymes caused the eosinophilic staining of the cytoplasm by showing the affinity of acidic dyes (eg, eosin, fuchsin) as a result of neutralizing RNA, structural and enzymatic cytoplasmic proteins [54].

An expression level of desmin is reported to be an important marker that reflects the severity of myocardial damage [55]. We observed that the Z lines of cardiomyocytes and desmin immunoreactivity levels were decreased in the ALD, SALD, AHD, and SAHD groups. The most dramatic decline was observed in the AHD group. Pawlak et al. noted that the remodeling of desmin cytoskeleton might contribute to the progression of idiopathic dilated cardiomyopathy and might affect patients' long-term prognosis [56].

It has been reported that pro-apoptotic proteins such as caspase-9, anti-apoptotic Bcl-2, and TUNEL-positive cell numbers are increased in an intrinsic apoptotic pathway (mitochondrial protein-mediated) [57, 58]. In the present study, BP decreased in proportion to the dose and duration of sPGe treatment. Reduced BP has been found to induce apoptotic death in cardiomyocytes whereas, increase myocardial caspase activity and TUNEL-positive apoptotic cell counts [59, 60]. It was thought that increased apoptotic activity in the SALD and AHD groups in our study may be due to the hypotensive effect of *Panax ginseng* [61].

It is well known that active caspase-9 then directly cleaves and activates effector caspases, such as caspase-3 [62]. While caspase immunoreactivity detects caspase expression in the tissue, the TUNEL method allows recognition of DNA strand breaks in cells. In the current study, TUNEL-positive cells increased in the SALD group, whereas caspase-9 immunoreactivity increased in the AHD group. Therefore, an increase in the caspase-9 activity in AHD group and an increase in TUNEL-positive cells in the SALD group may be due to this timely changing.

It is reported that *CAV1* is an important molecule [63] and that the decreasing *CAV1* expression may cause the structure of the caveola to deteriorate [64].

Conclusions

This experimental research results may fill the knowledge gaps in this field and contribute to universal knowledge. sPGe might induce cardiac pathologies including ST depression, T negativity, AV block and trigger a pathophysiology of diastolic dysfunction with low-dose use and increased the plasma concentration of cardiac troponin I without altering electrophysiological variables (PR, QRS, and QT interval). Thus, healthcare professionals should be aware of the cardiac effects of *Panax ginseng*. Well-designed clinical trials and more basic studies are needed to better understand the probable cardiac adverse effects of *Panax ginseng*. Our team is also studying the vascular effects of standardized *Panax ginseng* extract at an isolated organ bath system.

Acknowledgements This research is supported by a research grant from the Scientific and Technological Research Council of Turkey (Project details: 3001/115S818 belongs to Dr. Parlakpinar). Authors thank Azibe Yıldız, PhD for technical assistance and histological interpretation.

Author Contributions HP and AA are the coordinators of this study and they planned the study protocol design. LHT, HP, NE, and OO made the mandatory requirements for the study. LHT and OO were responsible for drug administration and data collection. HP and OO performed the surgical procedures. Hemodynamic parameters and cardiac results including ECG records were evaluated by NE and HP, NE performed the ECHO, LHT and OO conducted the biochemical analyses. The histopathological evaluations carried out by NV whereas YC performed genetic experiments. CC was responsible for data and statistical analysis and interpretation of the results. LHT was responsible for the design of figures and tables. This manuscript was written by HP, LHT, OO, NE, and YC The final manuscript is revised collaboratively by HP, LHT, and AA.

Compliance with Ethical Standards

Conflict of interest The author declares that they have no conflict of interests.

References

1. Gallin, J. I. (2017). A historical perspective on clinical research. In *Principles and practice of clinical research* (4th Ed.) (pp 1–15). Amsterdam: Elsevier.
2. Qi, Z., & Kelley, E. (2014). The WHO traditional medicine strategy 2014–2023: A perspective. *Science, 346*, S5–S6.
3. Choi, K. T. (2008). Botanical characteristics, pharmacological effects and medicinal components of Korean *Panax ginseng* CA Meyer. *Acta Pharmacologica Sinica, 29*, 1109–1118.
4. Karmazyn, M., Moey, M., & Gan, X. T. (2011). Therapeutic potential of ginseng in the management of cardiovascular disorders. *Drugs, 71*, 1989–2008.
5. Buettner, C., Yeh, G. Y., Phillips, R. S., Mittleman, M. A., & Kaptchuk, T. J. (2006). Systematic review of the effects of ginseng on cardiovascular risk factors. *Annals of Pharmacotherapy, 40*, 83–95.
6. Caron, M. F., Hotsko, A. L., Robertson, S., Mandybur, L., Kluger, J., & White, C. M. (2002). Electrocardiographic and hemodynamic effects of *Panax ginseng*. *Annals of Pharmacotherapy, 36*, 758–763.

7. Paik, D. J., & Lee, C. H. (2015). Review of cases of patient risk associated with ginseng abuse and misuse. *Journal of Ginseng Research, 39*, 89–93.
8. Park, B.-J., Lee, Y.-J., Lee, H.-R., Jung, D.-H., Na, H.-Y., Kim, H.-B., & Shim, J.-Y. (2012). Effects of Korean red ginseng on cardiovascular risks in subjects with metabolic syndrome: A double-blind randomized controlled study. *Korean Journal of Family Medicine, 33*, 190–196.
9. Vuksan, V., Stavro, M., Woo, M., Leiter, L., Sung, M., & Sievenpiper, J. (2006). Korean red ginseng (*Panax ginseng*) can lower blood pressure in individuals with hypertension: a randomized controlled trial, in *Proceedings of the 9th international ginseng symposium* (pp 25–28). Geumsan: Korean Society of Ginseng.
10. Kim, N. D., Kang, S. Y., & Schini, V. B. (1994). Ginsenosides evoke endothelium-dependent vascular relaxation in rat aorta. *General pharmacology, 25*, 1071–1077.
11. Kang, S. Y., Schini-Kerth, V. B., & Kim, N. D. (1995). Ginsenosides of the protopanaxatriol group cause endothelium-dependent relaxation in the rat aorta. *Life Sciences, 56*, 1577–1586.
12. Wagner, H., & Liu, X. (1987). *The international textbook of cardiology*. New York: Pergamon Press.
13. Turfan, M., Tasal, A., Ergun, F., & Ergelen, M. (2012). A sudden rise in INR due to combination of Tribulus terrestris, Avena sativa, and *Panax ginseng* (Clavis Panax). *Turk Kardiyoloji Dernegi arsivi: Turk Kardiyoloji Derneginin yayin organidir, 40*, 259–261.
14. Torbey, E., Rafeh, N. A., Khoueiry, G., Kowalski, M., & Bekheit, S. (2011). Ginseng: a potential cause of long QT. *Journal of Electrocardiology, 44*, 357–358.
15. Gunes, H., Kucukdurmaz, Z., Karapinar, H., & Gul, I. (2012). [Acute anterior myocardial infarction presented with cardiogenic shock in a patient on herbal medication]. *Turk Kardiyol Dern Ars, 40*, 262–264.
16. Martínez-Mir, I., Rubio, E., Morales-Olivas, F. J., & Palop-Larrea, V. (2004). Transient ischemic attack secondary to hypertensive crisis related to *Panax ginseng*. *Annals of Pharmacotherapy, 38*, 1970–1970.
17. Yüksel, I., Arslan, S., Çağırcı, G., & Yılmaz, A. (2013). Acute massive pulmonary embolism in a patient using clavis panax. *Turk Kardiyoloji Dernegi arsivi: Turk Kardiyoloji Derneginin yayin organidir, 41*, 351–353.
18. Parlakpinar, H., Ozhan, O., Ermis, N., & Acet, A. (2016). Cardiovascular effects of *Panax ginseng*. *Journal of Turgut Ozal Medical Center, 23*, 482–487
19. Zheng, M.-M., Xu, F.-X., Li, Y.-J., Xi, X.-Z., Cui, X.-W., Han, C.-C., & Zhang, X.-L. (2017). Study on transformation of ginsenosides in different methods. *BioMed Research International, 2017*, 8601027–8601027.
20. Wu, Y., Xia, Z., Dou, J., Zhang, L., Xu, J., Zhao, B., Lei, S., & Liu, H. (2011). Protective effect of ginsenoside Rb1 against myocardial ischemia/reperfusion injury in streptozotocin-induced diabetic rats. *Molecular Biology Reports, 38*, 4327–4335.
21. Jiang, Q.-S., Huang, X.-N., Dai, Z.-K., Yang, G.-Z., Zhou, Q.-X., Shi, J.-S., & Wu (2007). Inhibitory effect of ginsenoside Rb1 on cardiac hypertrophy induced by monocrotaline in rat. *Journal of Ethnopharmacology, 111*, 567–572.
22. Deng, J., Lv, X.-T., Wu, Q., & Huang, X.-N. (2009). Ginsenoside Rg1 inhibits rat left ventricular hypertrophy induced by abdominal aorta coarctation: involvement of calcineurin and mitogen-activated protein kinase signalings. *European Journal of Pharmacology, 608*, 42–47.
23. Liu, Z., Li, Z., & Liu, X.J. (2002). Effect of ginsenoside Re on cardiomyocyte apoptosis and expression of Bcl-2/Bax gene after ischemia and reperfusion in rats. *Journal of Huazhong University of Science and Technology [Medical Sciences], 22*, 305–309.
24. Li, J., Xie, Z.-Z., Tang, Y.-B., Zhou, J.-G., & Guan, Y.-Y. (2011). Ginsenoside-Rd, a purified component from panax notoginseng saponins, prevents atherosclerosis in apoE knockout mice. *European Journal of Pharmacology, 652*, 104–110.
25. McGrath, J., Drummond, G., McLachlan, E., Kilkenny, C., & Wainwright, C. (2010). Guidelines for reporting experiments involving animals: The ARRIVE guidelines. *British Journal of Pharmacology, 160*, 1573–1576.
26. Teichholz, L. E., Kreulen, T., Herman, M. V., & Gorlin, R. (1976). Problems in echocardiographic volume determinations: Echocardiographic-angiographic correlations in the presence or absence of asynergy. *The American journal of cardiology, 37*, 7–11.
27. Walker, M., Curtis, M., Hearse, D., Campbell, R., Janse, M., Yellon, D., Cobbe, S., Coker, S., Harness, J., & Harron, D. (1988). The Lambeth Conventions: Guidelines for the study of arrhythmias in ischaemia, infarction, and reperfusion. *Cardiovascular Research, 22*, 447–455.
28. Parlakpinar, H., Olmez, E., Acet, A., Ozturk, F., Tasdemir, S., Ates, B., Gul, M., & Otlu, A. (2009). Beneficial effects of apricot-feeding on myocardial ischemia-reperfusion injury in rats. *Food and Chemical Toxicology: An International Journal Published for the British Industrial Biological Research Association, 47*, 802–808.
29. Kalkan, F., Parlakpinar, H., Disli, O. M., Tanriverdi, L. H., Ozhan, O., Polat, A., Cetin, A., Vardi, N., Otlu, Y. O., & Acet, A. (2018). Protective and therapeutic effects of dexpanthenol on isoproterenol-induced cardiac damage in rats. *Journal of Cellular Biochemistry, 119*(9), 7479–7489
30. Ozbek, E., Simsek, A., Ozbek, M., & Somay, A. (2013). Caloric restriction increases internal iliac artery and penil nitric oxide synthase expression in rat: Comparison of aged and adult rats. *Archivio Italiano di Urologia e Andrologia, 85*, 113–117.
31. Livak, K. J., & Schmittgen, T. D. (2001). Analysis of relative gene expression data using real-time quantitative PCR and the 2-ΔΔCT method. *Methods, 25*, 402–408.
32. Curtis, M. J., Alexander, S., Cirino, G., Docherty, J. R., George, C. H., Giembycz, M. A., Hoyer, D., Insel, P. A., Izzo, A. A., Ji, Y., MacEwan, D. J., Sobey, C. G., Stanford, S. C., Teixeira, M. M., Wonnacott, S., & Ahluwalia, A. (2018). Experimental design and analysis and their reporting II: Updated and simplified guidance for authors and peer reviewers. *British Journal of Pharmacology, 175*, 987–993.
33. WSSPAS: Web-Based Sample Size & Power Analysis Software [Software]. (2018). Accessed Oct 01, 2018, from http://biostatapps.inonu.edu.tr/WSSPAS/.
34. Xiang, Y. Z., Shang, H. C., Gao, X. M., & Zhang, B. L. (2008). A comparison of the ancient use of ginseng in traditional Chinese medicine with modern pharmacological experiments and clinical trials. *Phytotherapy Research, 22*, 851–858.
35. Attele, A. S., Wu, J. A., & Yuan, C.-S. (1999). Ginseng pharmacology: Multiple constituents and multiple actions. *Biochemical Pharmacology, 58*, 1685–1693.
36. Zhou, W., Chai, H., Lin, P. H., Lumsden, A. B., Yao, Q., & Chen, C. (2004). Molecular mechanisms and clinical applications of ginseng root for cardiovascular disease. *Medical Science Monitor, 10*, RA187–RA192.
37. Cheng, Y., Shen, L. H., & Zhang, J. T. (2005). Anti-amnestic and anti-aging effects of ginsenoside Rg1 and Rb1 and its mechanism of action. *Acta Pharmacologica Sinica, 26*, 143–149.
38. Rhee, M.-Y., Cho, B., Kim, K.-I., Kim, J., Kim, M. K., Lee, E.-K., Kim, H.-J., & Kim, C.-H. (2014). Blood pressure lowering effect of Korea ginseng derived ginseol K-g1. *The American Journal of Chinese Medicine, 42*, 605–618.
39. Li, H.-X., Han, S.-Y., Ma, X., Zhang, K., Wang, L., Ma, Z.-Z., & Tu, P.-F. (2012). The saponin of red ginseng protects the cardiac

myocytes against ischemic injury in vitro and in vivo. *Phytomedicine, 19*, 477–483.
40. Jovanovski, E., Bateman, E. A., Bhardwaj, J., Fairgrieve, C., Mucalo, I., Jenkins, A. L., & Vuksan, V. (2014). Effect of Rg3-enriched Korean red ginseng (*Panax ginseng*) on arterial stiffness and blood pressure in healthy individuals: A randomized controlled trial. *Journal of the American Society of Hypertension, 8*, 537–541.
41. Lee, K. H., Bae, I. Y., Park, S. I., Park, J.-D., & Lee, H. G. (2016). Antihypertensive effect of Korean Red Ginseng by enrichment of ginsenoside Rg3 and arginine–fructose. *Journal of Ginseng Research, 40*, 237–244.
42. Lim, K. H., Ko, D., & Kim, J.-H. (2013). Cardioprotective potential of Korean Red Ginseng extract on isoproterenol-induced cardiac injury in rats. *Journal of Ginseng Research, 37*, 273.
43. Yan, X., Wu, H., Ren, J., Liu, Y., Wang, S., Yang, J., Qin, S., & Wu, D. (2018). Shenfu Formula reduces cardiomyocyte apoptosis in heart failure rats by regulating microRNAs. *Journal of Ethnopharmacology, 227*, 105–112.
44. Jin, Z., & Liu, C. (1994). Effect of ginsenoside Re on the electrophysiological activity of the heart. *Planta Medica, 60*, 192–193.
45. Jiang, M., Murias, J. M., Chrones, T., Sims, S. M., Lui, E., & Noble, E. G. (2014). American ginseng acutely regulates contractile function of rat heart. *Frontiers in Pharmacology, 5*, 43.
46. Nakaya, Y., Mawatari, K., Takahashi, A., Harada, N., Hata, A., & Yasui, S. (2007). The phytoestrogen ginsensoside Re activates potassium channels of vascular smooth muscle cells through PI3K/Akt and nitric oxide pathways. *The Journal of Medical Investigation: JMI, 54*, 381–384.
47. Komishon, A., Shishtar, E., Ha, V., Sievenpiper, J., de Souza, R., Jovanovski, E., Ho, H., Duvnjak, L. S., & Vuksan, V. (2016). The effect of ginseng (genus Panax) on blood pressure: A systematic review and meta-analysis of randomized controlled clinical trials. *Journal of Human Hypertension, 30*, 619.
48. Luo, D., & Fang, B. (2008). Structural identification of ginseng polysaccharides and testing of their antioxidant activities. *Carbohydrate Polymers, 72*, 376–381.
49. Ponikowski, P., Voors, A. A., Anker, S. D., Bueno, H., Cleland, J. G., Coats, A. J., Falk, V., González-Juanatey, J. R., Harjola, V. P., & Jankowska, E. A. (2016). 2016 ESC Guidelines for the diagnosis and treatment of acute and chronic heart failure: The Task Force for the diagnosis and treatment of acute and chronic heart failure of the European Society of Cardiology (ESC). Developed with the special contribution of the Heart Failure Association (HFA) of the ESC. *European Journal of Heart Failure, 18*, 891–975.
50. Afsin Oktay, A., & Shah, J., S (2015). Diagnosis and management of heart failure with preserved ejection fraction: 10 key lessons. *Current Cardiology Reviews, 11*, 42–52.
51. Disli, O. M., Sarihan, E., Colak, M. C., Vardi, N., Polat, A., Yagmur, J., Tamtekin, B., & Parlakpinar, H. (2013). Effects of molsidomine against doxorubicin-induced cardiotoxicity in rats. European surgical research. *Europaische chirurgische Forschung. Recherches chirurgicales europeennes, 51*, 79–90.
52. Parlakpinar, H., Ozer, M. K., & Acet, A. (2005). Effect of aminoguanidine on ischemia-reperfusion induced myocardial injury in rats. *Molecular and Cellular Biochemistry, 277*, 137–142.
53. Ozer, M. K., Parlakpinar, H., Vardi, N., Cigremis, Y., Ucar, M., & Acet, A. (2005). Myocardial ischemia/reperfusion-induced oxidative renal damage in rats: protection by caffeic acid phenethyl ester (CAPE). *Shock, 24*, 97–100.
54. Elmore, S. A., Dixon, D., Hailey, J. R., Harada, T., Herbert, R. A., Maronpot, R. R., Nolte, T., Rehg, J. E., Rittinghausen, S., & Rosol, T. J. (2016). Recommendations from the INHAND apoptosis/necrosis working group. *Toxicologic Pathology, 44*, 173–188.
55. Milner, D. J., Weitzer, G., Tran, D., Bradley, A., & Capetanaki, Y. (1996). Disruption of muscle architecture and myocardial degeneration in mice lacking desmin. *The Journal of Cell Biology, 134*, 1255–1270.
56. Pawlak, A., Gil, R., Kulawik, T., Pronicki, M., Karkucińska-Więckowska, A., Szymańska-Dębińska, T., Gil, K., Lagwinski, N., & Czarnowska, E. (2012). Type of desmin expression in cardiomyocytes—A good marker of heart failure development in idiopathic dilated cardiomyopathy. *Journal of Internal Medicine, 272*, 287–297.
57. Wang, Y., Xuan, L., Cui, X., Wang, Y., Chen, S., Wei, C., & Zhao, M. (2017). Ibutilide treatment protects against ER stress induced apoptosis by regulating calumenin expression in tunicamycin treated cardiomyocytes. *PLoS ONE, 12*, e0173469.
58. Colak, M., Parlakpinar, H., Tasdemir, S., Samdanci, E., Kose, E., Polat, A., Sarihan, E., & Acet, A. (2012). Therapeutic effects of ivabradine on hemodynamic parameters and cardiotoxicity induced by doxorubicin treatment in rat. *Human & Experimental Toxicology, 31*, 945–954.
59. Yuan, Y., Zhou, H., Wu, Q. Q., Li, F. F., Bian, Z. Y., Deng, W., Zhou, M. Q., & Tang, Q. Z. (2016). Puerarin attenuates the inflammatory response and apoptosis in LPS-stimulated cardiomyocytes. *Experimental and Therapeutic Medicine, 11*, 415–420.
60. Fujii, M., Sherchan, P., Soejima, Y., Doycheva, D., & Zhang, J. H. (2016). Subarachnoid hemorrhage-triggered acute hypotension is associated with left ventricular cardiomyocyte apoptosis in a rat model. In *Brain edema* XVI (pp 145–150). New York: Springer.
61. Riezzo, I., Centini, F., Neri, M., Rossi, G., Spanoudaki, E., Turillazzi, E., & Fineschi, V. (2009). Brugada-like EKG pattern and myocardial effects in a chronic propofol abuser. *Clinical Toxicology, 47*, 358–363.
62. Tanriverdi, L. H., Parlakpinar, H., Ozhan, O., Ermis, N., Polat, A., Vardi, N., Tanbek, K., Yildiz, A., & Acet, A. (2017). Inhibition of NADPH oxidase by apocynin promotes myocardial antioxidant response and prevents isoproterenol-induced myocardial oxidative stress in rats. *Free Radical Research, 51*, 772–786.
63. Couet, J., Belanger, M. M., Roussel, E., & Drolet, M. C. (2001). Cell biology of caveolae and caveolin. *Advanced Drug Delivery Reviews, 49*(3), 223–235.
64. Engelman, J. A., Zhang, X. L., Razani, B., Pestell, R. G., & Lisanti, M. P. (1999). p42/44 MAP Kinase-dependent and-independent Signaling Pathways Regulate Caveolin-1 Gene Expression. Activation of Ras-MAP kinase and protein kinase a signaling cascades transcriptionally down-regulates caveolin-1 promoter activity. *Journal of Biological Chemistry, 274*, 32333–32341.